

Critical spin dynamics of the $S = \frac{1}{2}$ spin chain compound CuSe_2O_5

K.-Y. Choi,¹ P. Lemmens,² and H. Berger³¹*Department of Physics, Chung-Ang University, 221 Huksuk-Dong, Dongjak-Gu, Seoul 156-756, Republic of Korea*²*Institute for Condensed Matter Physics, TU Braunschweig, D-38106 Braunschweig, Germany*³*Institute de Physique de la Matière Complexe, EPFL, CH-1015 Lausanne, Switzerland*

(Received 14 February 2011; revised manuscript received 30 March 2011; published 5 May 2011)

Phonon frequency and linewidth as well as quasielastic scattering due to spin energy fluctuations are used to evaluate the evolution of spin correlations in a spin chain system with considerable interchain coupling. In the compound CuSe_2O_5 these interactions lead to long-range order and a regime with enhanced classical critical dynamics. The resulting anomalies include the observation of quasielastic scattering intensity in interchain polarization, in addition to the usually reported intrachain polarization as well as the persistence of fluctuations to temperatures down below T_N . The inverse of the spin correlation length shows a linear temperature dependence with an offset at T_N . Finally, the derived magnetic contributions to the specific heat are pronounced around T_N while contributions due to one-dimensional fluctuations are hardly visible.

DOI: [10.1103/PhysRevB.83.174413](https://doi.org/10.1103/PhysRevB.83.174413)

PACS number(s): 78.35.+c, 75.10.Pq, 75.40.-s

I. INTRODUCTION

Quasi-one-dimensional (1D) $S = 1/2$ antiferromagnets have attracted much interest due to diverse ground states and pronounced quantum fluctuations.¹ Particularly, they provide a playground for testing fundamental theories of quantum magnetism.

An ideal $S = 1/2$ spin chain system shows no long-range ordering even at zero temperature owing to strong quantum fluctuations, although the spin-spin correlations decay algebraically along the chain.² Quite often, copper- and vanadium-based oxides with one hole (Cu^{2+} ; $3d^9$) or one electron (V^{4+} ; $3d^1$) realize quasi-1D $S = 1/2$ spin chains to good approximation. Remarkably, details of the crystal structure are known to be decisive in stabilizing the particular magnetic ground state of a transition-metal oxide. Prominent examples are the spin-Peierls ground state in CuGeO_3 ,³ the helical ground state in LiCuVO_4 ,⁴ and the noncollinear, incommensurate long-range-ordered state in LiCu_2O_2 .⁵ An accurate description of these phenomena necessitates an inclusion of correction terms to the isotropic Heisenberg Hamiltonian. Interchain interactions partially restore long-range magnetic ordering while intrachain frustration leads to a rich phase diagram.⁶⁻¹³

The magnetic behavior of weakly coupled $S = 1/2$ spin chains is largely described by a spin chain mean-field model, which provides a dichotomy between classical dynamics of the long-range-ordered state and critical dynamics of the quantum disordered state.^{10,11} Irkhin *et al.*¹⁴ showed that an inclusion of fluctuation corrections improves considerably the spin chain mean-field theory. Inelastic light scattering is widely recognized as one of the powerful experimental choices in addressing the dynamics of critical phenomena in such weakly coupled spin chains.¹ This is owing to an exceptionally effective coupling of light to the spin energy density, leading to a so-called quasielastic Raman response.¹⁵⁻¹⁹ This coupling permits us to obtain physical quantities such as the magnetic specific heat, the spin correlation length, and the magnetic contribution to a thermal conductivity, which is often impossible to gain using other experimental techniques.

In this respect, a light scattering study of the spin $S = 1/2$ Heisenberg spin chain compound CuSe_2O_5 will provide a deeper understanding on the critical spin dynamics in quasi-1D antiferromagnets and extend our knowledge of quasielastic Raman scattering to a spin chain with sizable interchain coupling.

The magnetic building block of the copper selenite CuSe_2O_5 is an isolated CuO_4 plaquette.²⁰⁻²³ The neighboring plaquettes are tilted with respect to each other and are arranged to form a dihedral angle $\varphi \approx 64^\circ$. They are bridged by Se_2O_5 polyanions, which are made of two SeO_3 pyramids sharing an oxygen atom. A structural chain is formed by an alternation of CuO_4 plaquettes and Se_2O_5 polyanion group along the c axis. Each spin chain is closely stacked in the b direction, and well separated in the a direction. Here we stress a structural peculiarity: The alternating arrangement of CuO_4 plaquettes does not permit longer-range interactions along the chain. Such interactions could have restricted and frustrated the evolution of spin correlations along the chain. In addition, further neighbor interactions are a prerequisite for Raman spin-exchange scattering at finite energies. In simple, nearest-neighbor-only spin chains the magnetic and the Raman spin-exchange Hamiltonian commute and finite-energy scattering is not observed.¹ Besides, from two short interchain coupling paths only one is relevant. That is, the interchain couplings are not frustrated. This leads to a simple description of the magnetic behavior of CuSe_2O_5 without any complications related to magnetic frustration.

Janson *et al.*²³ have extensively characterized the magnetic properties of CuSe_2O_5 by combining magnetic susceptibility, specific-heat measurements with a microscopic model. The magnetic susceptibility shows a broad maximum at $T_{\text{max}} \approx 101$ K and is well described by the Bethe ansatz, confirming one dimensionality. Band-structure calculations demonstrate that the minimal spin Hamiltonian of CuSe_2O_5 is captured by two exchange interaction parameters: the nearest-neighbor intrachain interaction of $J_c = 165$ K, which is weakened by a ferromagnetic Hund's rule coupling, and the nonfrustrated interchain interaction of $J_{ab} = 20$ K. Specific-heat measurements evidence an antiferromagnetic ordering at $T_N = 17$ K

and an additional distinct anomaly at 7 K of unknown origin. Unfortunately, it was not possible to resolve the magnetic contribution to the specific heat and respective entropy. Nevertheless the importance of interchain interactions is confirmed.

In our paper, we investigate phonon and magnetic excitations of the spin chain compound CuSe_2O_5 using inelastic light scattering, which is supplemented by a well-established set of arguments that should be relevant for quasi-1D spin systems. Our interest is to examine the applicability of the known theories to spin systems with a sizable, nonfrustrated interchain interaction and to compare that with results of frustrated spin chain and/or chains with much weaker interchain interactions. This will allow us to get insight into the critical spin dynamics of the studied system.

II. EXPERIMENTAL DETAILS

Single crystals of CuSe_2O_5 were grown by using a conventional chemical vapor transport method.²² For Raman measurements, single crystals with dimensions of $5 \times 0.5 \times 0.1 \text{ mm}^3$ were used. The samples were kept in the vacuum of an optical cryostat which is cooled by a closed-cycle refrigerator from room temperature down to 4 K. Raman scattering measurements were carried out in a quasibackscattering geometry with the excitation line $\lambda = 532 \text{ nm}$ of a Nd:yttrium aluminum garnet (YAG) solid-state laser. The incident power of 1 mW was focused to a 0.1-mm-diam spot on the surface of the single crystal. To fully suppress Rayleigh and stray light scatterings, a low-energy cutoff of Raman spectra was set to $\omega = 10 \text{ cm}^{-1}$. Raman spectra were collected in a range of $\omega = 10\text{--}1000 \text{ cm}^{-1}$ by a DILOR-XY triple spectrometer and a nitrogen-cooled charge-coupled device detector.

III. RESULTS AND DISCUSSION

A. Lattice dynamics and spin-phonon coupling

In quasi-1D spin systems Raman scattering experiments provide valuable information on lattice and spin dynamics through concomitant excitations of lattice vibrations and magnetic modes. The coupling of lattice and spin degrees of freedom might cause phonon anomalies, and the coupling of light to the spin energy density leads to quasielastic scattering. In the following we will address both aspects in the $S = 1/2$ Heisenberg spin chain compound CuSe_2O_5 .

Figure 1 shows Raman spectra at 4 and 293 K in (*cc*), (*aa*), and (*ac*) polarizations, respectively. In the (*cc*) and (*aa*) polarization where incident and scattered light polarizations are parallel to the *c* and *a* axis, respectively, we observe nine phonon modes, which have exactly the same energies in both polarizations. In the (*ac*) polarization where the incident (scattered) light is polarized parallel (perpendicular) to the chain direction, we also observe nine phonon modes whose energies are shifted systematically by 10–40 cm^{-1} as compared to those of the parallel polarizations. A careful analysis of the spectra unveils that two phonon modes are grouped either within the same polarization or with other polarizations with the energy difference of 10–30 cm^{-1} . For example, the 156 and 173 cm^{-1} modes in the (*cc*) polarization are grouped together, the 308 and 336 cm^{-1} modes in the (*ac*)

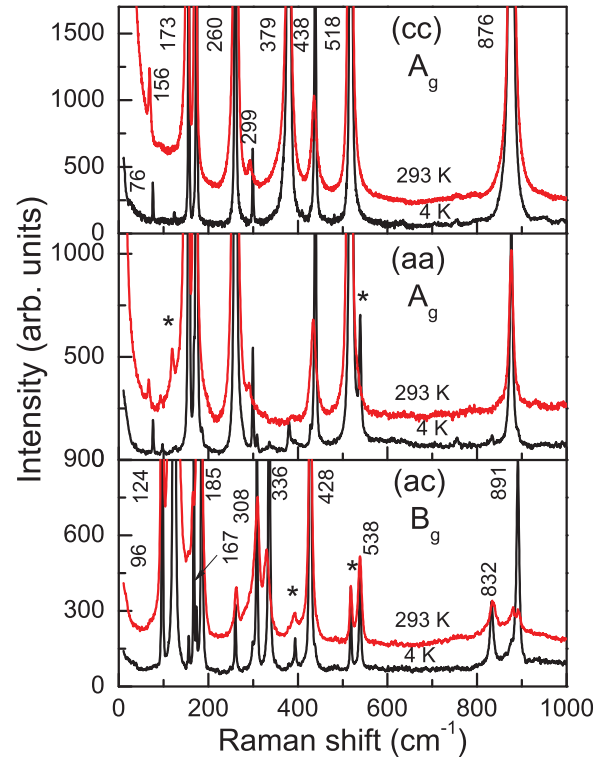


FIG. 1. (Color online) Comparison of Raman spectra of CuSe_2O_5 at 4 and 293 K in (*cc*), (*aa*), and (*ac*) polarizations, in the respective upper, middle, and lower panels. The numbers denote the energies of phonon modes allowed in the parallel and crossed polarization, respectively. The asterisks indicate weak forbidden modes. The spectra are shifted for clarity.

polarization, and the 518 and 538 cm^{-1} modes in the (*ac*) and (*cc*) polarization, respectively.

According to the symmetry analysis of the monoclinic space group, $C2/c$, oxygen atoms possess three crystallographically different sites. Two of them occupy the same Wyckoff position $8f$ and thereby give $3A_g$ and $3B_g$ Raman-active modes. In the present scattering geometry the A_g symmetry modes are expected in the (*cc*) and (*aa*) polarizations while the B_g modes are in the (*ac*) polarization. Since copper atoms occupying the $4b$ position are not involved in Raman-active modes, two oxygen modes with the same Wyckoff position but with a different crystallographic site will appear pairwise with an almost equal energy separation as described above. Taking into account the Se ($8f$) atoms, we expect a total of $\Gamma_{\text{Raman}} = 9A_g(aa, bb, cc, ab) + 9B_g(ac, bc)$ Raman-active modes. We were able to detect a sum of 18 phonon modes as predicted by the factor group analysis. We note the observation of additional weak modes (see the asterisks in Fig. 1). They are identified to show up due to a leakage of a selection rule, and judging from that they have corresponding partner modes with the same frequency and strong scattering intensity in different polarizations.

For quasi-1D antiferromagnets, particularly with low lattice symmetry, ionic displacements do not cancel each other in modulating magnetic exchange paths, and thus optical phonons can be used to probe a change of spin degrees of freedom.¹ With this in mind, we carry out a detailed analysis

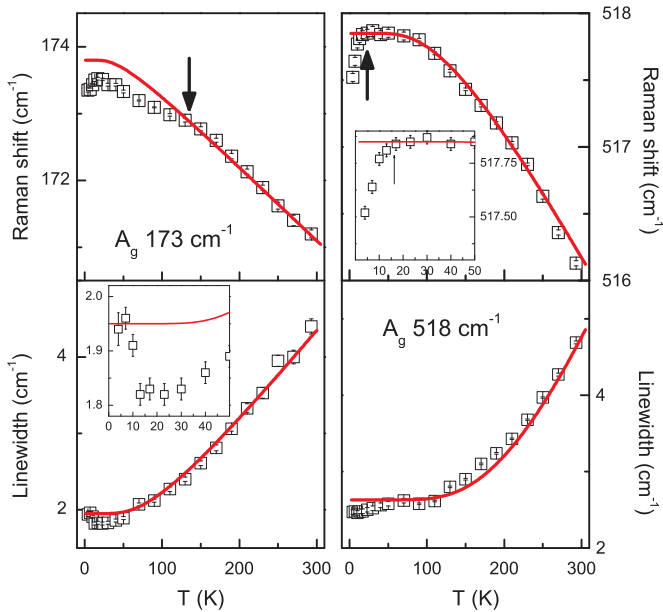


FIG. 2. (Color online) Temperature dependence of the peak position and the linewidth of two A_g phonon modes at 173 cm^{-1} (left-hand panel) and 518 cm^{-1} (right-hand panel). The solid lines represent a fit to Eqs. (1) and (2), respectively. The characteristic temperatures, which show anomalous phonon energy behavior, are indicated by arrows. The insets focus on the low-temperature regime.

of the phonon frequencies and linewidths. Concerning the temperature dependence of the phonon modes, we observe a small hardening of frequency by $2\text{--}4 \text{ cm}^{-1}$ and a moderate damping but no substantial change of the scattering intensity.

Figure 2 summarizes the temperature dependence of frequency and linewidth of the 173 and 518 cm^{-1} modes. The error bars are smaller than the symbol size and thus are hardly visible. Both modes with lower and higher frequencies exhibit a frequency hardening by $\sim 2 \text{ cm}^{-1}$ and a moderate narrowing of linewidth by 3 cm^{-1} with decreasing temperature. Noticeably, a small but discernible softening is found for temperatures below $\sim 17 \text{ K}$, the antiferromagnetic ordering temperature. This gives evidence for spin-phonon couplings. Such spin-phonon interactions are very pronounced in low-dimensional spin dimer systems, as reported in CuGeO_3 as well as in two- and three-dimensional frustrated spin systems $\text{SrCu}_2(\text{BO}_3)_2$ and ZnCr_2O_4 , respectively.^{24–26} Compared to frustrated spin systems, however, the phonon anomalies caused by spin-phonon coupling are marginal for the studied system. Although these effects are small, we can still extract important information about spin-spin correlation functions.

In order to differentiate any contribution of spin-phonon coupling to the frequency shift, we have calculated the anharmonic phonon contribution based on phonon-phonon decay processes to acoustic phonons,²⁷

$$\omega_{\text{ph}}(T) = \omega_0 + A \left(1 + \frac{2}{e^x - 1} \right), \quad (1)$$

where $x = \hbar\omega_0/2k_B T$ and constant A . Here, ω_0 is the frequency of the optical mode at zero temperature. The high-frequency mode at 518 cm^{-1} is well fitted by Eq. (1) with values of $\omega_0 = 519.9 \text{ cm}^{-1}$ and $A = -2.08 \text{ cm}^{-1}$ except

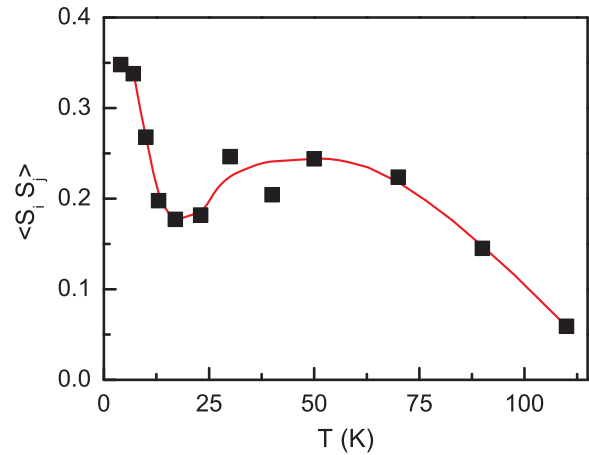


FIG. 3. (Color online) Temperature dependence of the spin-spin correlation functions obtained by subtracting the frequency of the 173 cm^{-1} mode from the fitted value to Eq. (1). The line is a guide to the eye.

for a small softening for temperatures below 17 K , as indicated by the arrow. However, the low-frequency mode at 173 cm^{-1} is not reasonably well described in the whole temperature range. Since in the high-temperature limit the temperature dependence of the phonon frequency is approximated as linear, $\omega_{\text{ph}}(T) \propto T$, we restrict the fitting range to temperatures above 110 K . The fitted curve with values of $\omega_0 = 174.5 \text{ cm}^{-1}$ and $A = -0.72 \text{ cm}^{-1}$ is denoted by the solid line. The deviation is clearly visible for temperatures below 100 K . The onset temperature coincides with the broad maximum in the magnetic susceptibility, which heralds the development of short-range correlations. This supports a coupling of the lattice to spin degrees of freedom.¹ The temperature dependence of the phonon linewidth is analyzed by using²⁷

$$\Gamma(T) = \Gamma_0 \left(1 + \frac{B}{e^y - 1} \right), \quad (2)$$

where $y = \hbar\omega_0/k_B T$ with the frequency ω_0 of the phonon mode. We obtain an overall agreement between the experimental data and the fitted lines, although there appear small discrepancies at low temperatures.

The spin-induced phonon frequency shift based on the Baltensperger and Helman model²⁸ has been well established and successfully applied to diverse magnetic systems to explain renormalizations of phonon energy induced by the magnetic energy of the system. According to them, the phonon frequency shift is related to the scalar spin correlation function, i.e., $\Delta\omega \approx \lambda \langle S_i S_j \rangle$, where λ is the spin-phonon coupling parameter. Here we note that λ is given by the second derivatives of the coupling energy with respect to the atomic displacements. We obtain the spin-spin correlation function by subtracting the estimated anharmonic shift given by Eq. (1) from the frequency of the 173 cm^{-1} mode as a function of temperature. The result is shown in Fig. 3. Upon cooling from 110 K the spin-spin correlation function slowly increases and shows a kink at $\sim 17 \text{ K}$. The onset temperature lies in the temperature interval where the magnetic susceptibility shows a broad maximum. The steep increase of $\langle S_i S_j \rangle$ seems to be correlated with antiferromagnetic ordering.

B. Quasielastic scattering and critical spin dynamics

In quasi-1D antiferromagnets, quasielastic light scattering can probe the critical spin dynamics. Two different mechanisms have been discussed. One is due to diffusive fluctuations of a four-spin time correlation function.²⁹ In this case, the quasielastic scattering is approximated by a Gaussian-like spectral function.^{18,19} The other relies on fluctuations of the magnetic energy density.¹⁶ It turns out that the latter is mainly responsible for the low-energy scattering near a zero-frequency shift region observed in LiCu_2O_2 , CuGeO_3 , and KCuF_3 .^{5,30,31} In the following, thus, we will summarize the well-established theories before discussing the experimental data. According to Reiter and Halley,^{16,17} a two-spin process leads to scattering intensity for temperatures above the critical temperature;

$$I(\omega) \propto \int_{-\infty}^{\infty} e^{-i\omega t} dt \langle E(k,t)E^*(k,0) \rangle, \quad (3)$$

where $E(k,t)$ is a magnetic energy density given by the Fourier transform of $E(r) = -\langle \sum_{i>j} J_{ij} S_i \cdot S_j \delta(r - r_i) \rangle$ with the position of the i th spin r_i . Applying the fluctuation-dissipation theorem in the hydrodynamic limit,¹⁷ Eq. (3) is simplified to

$$I(\omega) \propto \frac{\omega}{1 - e^{-\beta\hbar\omega}} \frac{C_m T D k^2}{\omega^2 + (Dk^2)^2}, \quad (4)$$

where $\beta = 1/k_B T$, C_m is the magnetic specific heat, and D is the thermal diffusion constant $D = K/C_m$ with the magnetic contribution to the thermal conductivity K . Equation (4) can be reformulated in terms of a Raman susceptibility $\chi''(\omega)$,

$$\frac{\chi''(\omega)}{\omega} \propto C_m T \frac{Dk^2}{\omega^2 + (Dk^2)^2}. \quad (5)$$

In the high-temperature limit, Eq. (4) further simplifies to a Lorentzian profile,

$$I(\omega) \propto C_m T^2 \frac{Dk^2}{\omega^2 + (Dk^2)^2}. \quad (6)$$

Equations (5) and (6) imply that the magnetic specific heat and thermal diffusion constant can be obtained from either the Raman scattering intensity $I(\omega)$ or the Raman susceptibility divided by the frequency $\chi''(\omega)/\omega$. Furthermore, we note that both quantities have the same Lorentzian spectral function but with different temperature-dependent proportional constants.

In the following we will analyze the low-energy Raman spectra in terms of Eqs. (5) and (6) and compare these results. Figure 4(a) shows the temperature dependence of the quasielastic response. The scattering intensity is drastically reduced with decreasing temperature from 293 K. The observed spectra are equally well fitted to both Eqs. (5) and (6) at room temperature [see Figs. 4(b) and 4(c)]. As can be seen from Fig. 4(b), we observe also a substantial quasielastic response in the interchain polarization, namely, in the (*aa*) polarization. The ratio of the interchain to the intrachain scattering intensity amounts to $I^{(aa)}/I^{(cc)} \approx 1/7$. To the best of our knowledge, for quasi-1D spin systems such a quasielastic scattering has only been reported experimentally with intrachain light polarization. The presence of the interchain quasielastic response should be ascribed to a sizable interchain coupling. Noticeably, the intensity ratio is very close to that of the calculated

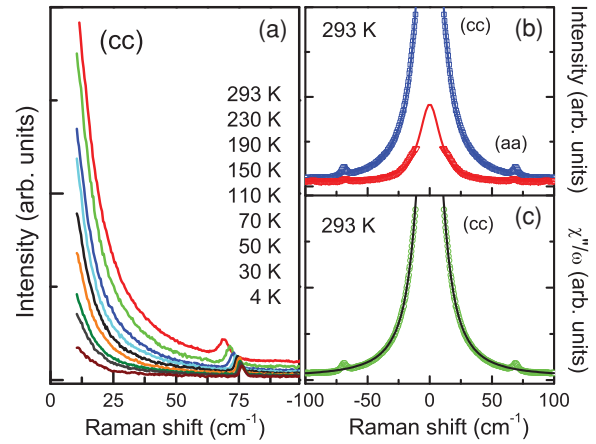


FIG. 4. (Color online) (a) Temperature dependence of quasielastic scattering in (*cc*) polarization at low frequencies. (b) Comparison of the quasielastic scattering between (*cc*) and (*aa*) polarizations at 293 K. (c) The Raman response $\chi''(\omega)/\omega$ at 293 K. The solid lines are fits to Lorentzian curves given by Eqs. (5) and (6).

interchain to intrachain exchange interaction $J^{ab}/J^c \approx 1/8$.²³ Besides, we find a nonnegligible spectral weight even below T_N . In the magnetic ordered state one should take into account the contribution to the scattering intensity due to magnetization and possibly diffusive spin fluctuations as well.¹⁶ In this case, the observed quasielastic scattering below T_N is made of several different contributions and thus should be analyzed by assuming either two Lorentzian lines or a sum of two Lorentzian lines and one Gaussian line.³² We fail to obtain a reliable set of parameters because the scattering intensity is weak and the spectra are not available for frequencies below 10 cm^{-1} . Therefore, our analysis is restricted to temperatures above T_N .

As discussed above, quasielastic scattering provides two important parameters: the inverse of the spin correlation length ξ^{-1} and the magnetic specific heat C_m . Figure 5(a) shows the temperature dependence of $\Gamma(T) \propto \xi^{-1}$, which is obtained by the full width at half maximum of two Lorentzian profiles, Eqs. (5) and (6), respectively. Since the scattering intensity of $I(T) [\chi''(T)/\omega]$ is proportional to $C_m T^2 [C_m T]$, the magnetic specific heat is derived by exploiting the relation $C_m \propto I(T)/T^2 [\chi''(T)/\omega T]$. In Fig. 5(b) we show the temperature dependence of C_m calculated by two different methods.

We will first discuss the detailed temperature dependence of $\Gamma(T)$. The linewidth obtained from $\chi''(T)/\omega$ shows a close to linear T dependence while that from Eq. (6) exhibits a deviation from linearity at ~ 110 K. Assuming a mean-field T dependence of C_m , one expects a linear T dependence of $\Gamma(T) \propto (T - T_N)$.^{33,34} In our case, $\Gamma(T)$ still has a finite value at T_N . This is explained by noting the relation $\Gamma(T) \propto K/C_m$, where K is governed by short-range correlations while C_m is dominated by long-range ordering.¹⁷ In a quasi-1D spin system the specific heat will not diverge at a critical point so that $\Gamma(T)$ will not go to zero at T_N . In this light, the deviation from linearity at ~ 110 K implies a breakdown of the high-temperature approximation. Therefore, one should be careful in applying the simplified Eq. (6) to moderately coupled spin chains in the low-temperature regime.

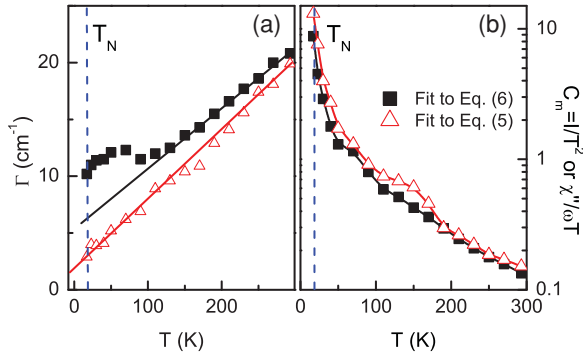


FIG. 5. (Color online) Temperature dependence of linewidth Γ (a) and magnetic specific heat C_m on a logarithmic scale (b). The full square (open triangle) symbols stand for the parameters extracted from a fit to Eq. (5) [Eq. (6)]. The solid lines are guides to the eye and the vertical dashed lines indicate the magnetic ordering temperature T_N . Details are described in the text.

Next we turn to the temperature dependence of C_m . To discriminate any difference between the two procedures, C_m is plotted on a logarithmic scale. They show a similar behavior: Approaching the critical temperature T_N the magnetic specific heat increases steeply. However, we notice that C_m derived by the high-temperature approximation tends to be systematically underestimated for temperatures below 180 K. Although there is some indication for an enhanced specific heat starting from 180 K, we cannot identify a discernible maximum in the temperature range $0.48J_c \approx 80\text{--}90$ K, which is expected for a 1D Heisenberg chain.^{23,24,35} The same observation has been made in the analysis of the specific heat using a conventional thermodynamic method and attributed to a dominating lattice contribution.²³ For our analysis this argument does not hold. Therefore we conclude that below 100 K the specific heat is dominated by a classical spin dynamics, leading to long-range ordering, and thus the maximum of C_m characteristic for a 1D quantum critical dynamics is obscured by magnetic degrees of freedom.^{35,36}

Finally, we remark on the specific-heat anomaly at 7 K reported by thermodynamic techniques.²³ As mentioned above, for temperatures below T_N we cannot calculate C_m

unambiguously and thus cannot give quantitative arguments. Nonetheless, the persistence of quasielastic scattering below T_N suggests the presence of diffusive type of spin fluctuations and/or spin-energy fluctuations in this *ordered* state. The order at T_N is therefore not related to a total release of spin entropy and further ordering phenomena, i.e., a transition into a canted spin state, could take place. To fully resolve this issue, quasielastic scattering should be studied near the zero-frequency regime ($\omega < 10\text{ cm}^{-1}$) using a Brillouin spectrometer.

IV. CONCLUSIONS

We presented a Raman scattering study of the quasi-one-dimensional spin compound CuSe_2O_5 . This system is characterized by a moderate, nonfrustrated interchain coupling $J^{ab}/J^c \approx 1/8$ and a sizable magnetic ordering temperature scale of $T_N/J^c \approx 0.1$.²³ With the help of the phonon frequency renormalization induced by spin-phonon coupling, we extract the spin-spin correlation function, which shows a slow increase with decreasing temperature from 110 K and a steep increase at ~ 17 K. In the quasielastic scattering channel we find several distinct features: (i) an appreciable scattering intensity in the interchain polarization in addition to the strong intrachain one, (ii) the persistence of the quasielastic scattering down below T_N , (iii) the linear T dependence of $\Gamma(T)$ with a finite offset at T_N , and (iv) the predominance of classical critical spin dynamics over spin chain correlations in their contribution to C_m . To the best of our knowledge, these are not known from previous investigations in weakly coupled or dimerized spin chains. The key factor is a sizable inter-chain coupling without frustration, which enhances the classical dynamics with respect to the quantum disordered spin dynamics of a 1D quantum magnet.

ACKNOWLEDGMENTS

K.Y.C. acknowledges financial support from the Alexander-Humboldt Foundation and the Priority Research Center Program funded by NRF Grant No. 2009-0093817. Part of the work was supported by DFG, IHRP, and the EIEG program.

¹P. Lemmens, G. Güntherodt, and C. Gros, *Phys. Rep.* **375**, 1 (2003).

²H. Bethe, *Z. Phys.* **71**, 205 (1931).

³M. Hase, I. Terasaki, and K. Uchinokura, *Phys. Rev. Lett.* **70**, 3651 (1993).

⁴M. Enderle, C. Mukherjee, B. Fåk, R. K. Kremer, J.-M. Broto, H. Rosner, S.-L. Drechsler, J. Richter, J. Malek, A. Prokofiev, W. Assmus, S. Pujol, J.-L. Raggazzoni, H. Rakoto, M. Rheinstädter, and H. M. Rønnow, *Europhys. Lett.* **70**, 237 (2005).

⁵K.-Y. Choi, S. A. Zvyagin, G. Cao, and P. Lemmens, *Phys. Rev. B* **69**, 104421 (2004).

⁶D. J. J. Farnell and J. B. Parkinson, *J. Phys. Condens. Matter* **6**, 5521 (1994).

⁷K. Okamoto and K. Nomura, *Phys. Lett. A* **169**, 433 (1992).

⁸R. Chitra, S. Pati, H. R. Krishnamurthy, D. Sen, and S. Ramasesha, *Phys. Rev. B* **52**, 6581 (1995).

⁹T. Tonegawa and I. Harada, *J. Phys. Soc. Jpn.* **58**, 2902 (1989).

¹⁰H. J. Schulz, *Phys. Rev. Lett.* **77**, 2790 (1996).

¹¹F. H. L. Essler, A. M. Tsvelik, and G. Delfino, *Phys. Rev. B* **56**, 11001 (1997).

¹²C. Yasuda, S. Todo, K. Hukushima, F. Alet, M. Keller, M. Troyer, and H. Takayama, *Phys. Rev. Lett.* **94**, 217201 (2005).

¹³A. A. Zvyagin and S.-L. Drechsler, *Phys. Rev. B* **78**, 014429 (2008).

¹⁴V. Yu. Irkhin and A. A. Katanin, *Phys. Rev. B* **61**, 6757 (2000).

¹⁵G. F. Reiter, *Phys. Rev. B* **13**, 169 (1976).

¹⁶J. W. Halley, *Phys. Rev. Lett.* **41**, 1605 (1978).

¹⁷B. I. Halperin and P. C. Hohenberg, *Phys. Rev.* **188**, 898 (1969).

¹⁸W. J. Brya and P. M. Richards, *Phys. Rev. B* **9**, 2244 (1974).

¹⁹P. M. Richards and W. J. Brya, *Phys. Rev. B* **9**, 3044 (1974).

²⁰G. Meunier, C. Svenssen, and A. Darpy, *Acta Crystallogr. Sect. B* **32**, 2664 (1976).

- ²¹O. Kahn, M. Verdagner, J. J. Girerd, J. Galy, and F. Maury, *Solid State Commun.* **34**, 971 (1980).
- ²²R. Becker and H. Berger, *Acta Crystallogr. E* **62**, i256 (2006).
- ²³O. Janson, W. Schnelle, M. Schmidt, Yu. Prots, S.-L. Drechsler, S. K. Filatov, and H. Rosner, *New J. Phys.* **11**, 113034 (2009).
- ²⁴M. Braden, B. Hennion, W. Reichardt, G. Dhalenne, and A. Revcolevschi, *Phys. Rev. Lett.* **80**, 3634 (1998).
- ²⁵K.-Y. Choi, Yu. G. Pashkevich, K. V. Lamonova, H. Kageyama, Y. Ueda, and P. Lemmens, *Phys. Rev. B* **68**, 104418 (2003).
- ²⁶Ch. Kant, J. Deisenhofer, T. Rudolf, F. Mayr, F. Schrettle, A. Loidl, V. Gnezdilov, D. Wulferding, P. Lemmens, and V. Tsurkan, *Phys. Rev. B* **80**, 214417 (2009).
- ²⁷M. Balkanski, R. F. Wallis, and E. Haro, *Phys. Rev. B* **28**, 1928 (1983).
- ²⁸W. Baltensperger and J. S. Helman, *Helv. Phys. Acta* **41**, 668 (1968).
- ²⁹P. H. M. van Loosdrecht, J. P. Boucher, G. Martinez, G. Dhalenne, and A. Revcolevschi, *Phys. Rev. Lett.* **76**, 311 (1996).
- ³⁰H. Kuroe, J. I. Sasaki, T. Sekine, N. Koide, Y. Sasago, K. Uchinokura, and M. Hase, *Phys. Rev. B* **55**, 409 (1997).
- ³¹I. Yamada and H. Onda, *Phys. Rev. B* **49**, 1048 (1994).
- ³²If quasielastic scattering contains two contributions from fluctuations of the spin energy density and a parallel component of the sublattice magnetization, it is described by a sum of two Lorentzian profiles. If diffusive fluctuations are present, a Gaussian profile should be added.
- ³³K. Kawasaki, *Phys. Rev.* **150**, 291 (1966).
- ³⁴K. Kawasaki and M. Tanaka, *Proc. Phys. Soc. London* **90**, 791 (1967).
- ³⁵D. C. Johnston, R. K. Kremer, M. Troyer, X. Wang, A. Klumper, S. L. Bud'ko, A. F. Panchula, and P. C. Canfield, *Phys. Rev. B* **61**, 9558 (2000).
- ³⁶In a limited temperature regime above T_N a scaling of the specific heat can be investigated according to $\Delta C_m \sim (T/T_N)^\mu$. We found for both data sets $\mu = 0.28$. This value is close to what is expected for a 3D $S = 1/2$ Heisenberg model.